land

MDPI

Article

Spatio-Temporal Change in Urban Carbon Metabolism Based on Ecological Network Analysis: A Case Study in the Beijing–Tianjin–Hebei Urban Agglomeration, China

Fang Xu * and Xiaoyou Guo

School of Landscape Architecture, Beijing Forestry University, Beijing 100083, China; xiaoyou@design.upenn.edu
* Correspondence: fangxu2019@bjfu.edu.cn

Abstract: Urban carbon emissions significantly contribute to climate change, exacerbating environmental issues such as global warming. Understanding carbon metabolism is vital for identifying key emission sources and implementing targeted mitigation strategies. This study presents an innovative carbon metabolism analysis framework that integrates an ecological network analysis (ENA) with land use dynamics, enriching the theoretical system and providing policy recommendations for sustainable urban development. We investigated carbon metabolism in the Beijing–Tianjin–Hebei Urban Agglomeration (BTHUA) from 2000 to 2020 using land use and statistical data. The ENA method quantified the ecological relationships between land use compartments. Our findings revealed that industrial and transportation land exhibited the highest carbon emission density, while forest land demonstrated the highest carbon sequestration density. Notably, the negative net horizontal carbon flow indicated that land use changes exacerbated the disorder of carbon metabolism. The increasing mutualism index suggested a reduction in the negative impacts of land use changes on carbon metabolism. This study highlights the importance of spatial planning in transforming ecological relationships and provides a comprehensive understanding of carbon metabolism dynamics influenced by land use changes. The insights gained can inform effective mitigation strategies in the BTHUA and similar urban agglomerations, ultimately contributing to sustainable urban development.

Keywords: urban carbon metabolism; land use and land cover change (LUCC); ecological network analysis (ENA); urban agglomeration

check for updates

Citation: Xu, F.; Guo, X. Spatio-Temporal Change in Urban Carbon Metabolism Based on Ecological Network Analysis: A Case Study in the Beijing–Tianjin–Hebei Urban Agglomeration, China. *Land* **2024**, *13*, 2252. https://doi.org/10.3390/land13122252

Academic Editor: Xuechao Wang

Received: 10 October 2024
Revised: 2 December 2024
Accepted: 18 December 2024
Published: 23 December 2024

Copyright: © 2024 by the authors. Licensee MDPI, Basel, Switzerland. This article is an open access article distributed under the terms and conditions of the Creative Commons Attribution (CC BY) license (https://creativecommons.org/licenses/by/4.0/).

1. Introduction

Rapid urbanization and industrialization are transforming landscapes globally, driving profound environmental changes, particularly concerning greenhouse gas emissions and climate change [1]. Urban areas, despite occupying a small fraction of the Earth's surface, contribute disproportionately to global greenhouse gas emissions, largely due to land use and land cover changes [2]. The conversion of natural landscapes, such as forests and grasslands, to built-up areas diminishes the carbon sequestration capacity and fundamentally alters carbon metabolism at the local and regional scales [3]. This dynamic interplay between urban development and environmental sustainability is particularly evident in rapidly developing nations like China.

China, which is experiencing unprecedented urbanization, faces the dual challenge of fostering economic growth while mitigating environmental impacts [4]. The Beijing–Tianjin–Hebei Urban Agglomeration (BTHUA), one of the most developed and populous regions in China, exemplifies this challenge [5]. The region's coal-based energy structure and industrial activities dominated by energy-intensive industries have led to substantial carbon dioxide emissions. From 2000 to 2019, the total carbon emissions in the BTHUA increased from 360 million tons to 1.16 billion tons, accounting for over 10% of China's total carbon emissions [6]. Understanding the urban carbon metabolism in this region, which encompasses the exchanges of carbon between the natural environment and human

activities, is crucial for developing effective regional climate change mitigation strategies [7]. Specifically, quantifying the current state of carbon emissions in the BTHUA is essential for establishing a baseline against which mitigation efforts can be measured. Recent data indicate that the BTHUA continues to be a significant emitter, highlighting the urgent need for targeted interventions [8].

Land use change has been identified as a primary driver of carbon storage loss and a significant contributor to urban carbon metabolism [9]. The conversion of high carbon storage density land, such as forests and grassland, to built-up land with low carbon storage densities, has led to a net increase in atmospheric CO_2 levels [10]. Understanding the spatio-temporal dynamics of urban carbon metabolism is essential for developing effective land-based mitigation policies [11].

The study of urban carbon metabolism has evolved significantly. Early research focused on basic carbon accounting using methods like field surveys [12], process-based models [13], remote sensing [14], and emission factor approaches [15]. These studies provided fundamental insights into urban carbon cycling [16]. Subsequent research expanded the scope to encompass the impacts of various land uses on carbon emissions and sequestration [17–19]. This shift towards a holistic ecosystem perspective, considering the coupled natural and socio-economic processes, has advanced our understanding of urban carbon dynamics [20]. However, there remains a need for a comprehensive understanding of the integrated effects of LULCC on urban carbon metabolism. Few studies have examined the systemic interactions and ecological relationships within these metabolic networks [3,21].

Ecological network analysis (ENA) is an effective tool for describing the state, structure, function, and transformation of ecosystems [22]. Initially applied to natural systems, ENA has been extended to socio-economic systems, revealing the principles of interaction between metabolic components in urban ecosystems [23]. Network utility analysis, a method within ENA, uncovers the nature of relationships between components and explains the relative gains and losses within interactive networks [24]. This approach allows for a more nuanced understanding of the complex interplay between land use changes and carbon flows. Despite its potential, the integration of ENA with urban carbon metabolism research remains relatively unexplored. This study aims to bridge this gap by leveraging ENA to analyze the ecological relationships within the BTHUA's carbon metabolism network. This approach goes beyond simply quantifying carbon flows, as it delves into the underlying ecological relationships driving these flows, offering a more comprehensive understanding of the system's dynamics [25].

Furthermore, existing research on urban carbon metabolism has predominantly focused on developed countries, overlooking the unique challenges faced by rapidly urbanizing regions in developing countries like China [20,26]. These regions often experience rapid, large-scale land transformations with significant implications for carbon dynamics. This study addresses this gap by focusing on the BTHUA, a representative case of rapid urbanization in a developing country context. By integrating ENA with a carbon metabolism analysis, we aim to provide a more nuanced understanding of the ecological relationships between land use components, informing targeted policy interventions.

This study presents an innovative framework that integrates a carbon metabolism analysis with ENA to assess the spatio-temporal changes in urban carbon metabolism within the BTHUA. This integrated approach allows for a systematic evaluation of the complex interactions between different urban land use types and their associated carbon flows, providing a more holistic understanding of urban carbon dynamics. Specifically, this study advances existing research by (1) explicitly incorporating ENA to analyze the ecological relationships within the carbon metabolism network, moving beyond the simple quantification of carbon flows; and (2) providing targeted policy recommendations based on the identified ecological relationships.

The specific objectives of this study are to (1) quantify the spatio-temporal patterns of carbon emissions and sequestration within the BTHUA from 2000 to 2020; (2) evaluate the ecological relationships and network structure influencing carbon metabolism using ENA;

and (3) provide policy recommendations for enhancing carbon efficiency and sustainability within the urban agglomeration. The remainder of this paper is structured as follows: Section 2 details the materials and methods employed, including data sources and the ENA framework. Section 3 presents the results of the analysis, followed by a discussion of the findings in Section 4. Finally, Section 5 concludes the study and outlines future research directions. By addressing these objectives, this study contributes to a deeper understanding of urban sustainability and offers practical insights for developing low-carbon urban strategies in the BTHUA and similar urban clusters worldwide.

2. Materials and Methods

2.1. Study Area

The BTHUA (113°04′–119°53′ E, 36°01′–42°37′ N, Figure 1) is located in the northern part of the North China Plain, covering an area of 218,000 km^2 [27]. This region is characterized by a continental monsoon climate, with annual sunshine durations ranging from 2500 to 2900 h, average annual temperatures between 8 °C and 12.5 °C, and annual precipitation of about 800 mm [28]. The BTHUA comprises 13 cities, including Beijing and Tianjin, as well as 11 cities in Hebei Province. The population of the BTHUA reached approximately 109.43 million in 2023, accounting for about 7.76% of China's total population [29]. The region serves as a critical economic hub, but its rapid urbanization and industrial growth have resulted in significant carbon emissions, necessitating comprehensive environmental impact assessments and mitigation strategies [4].

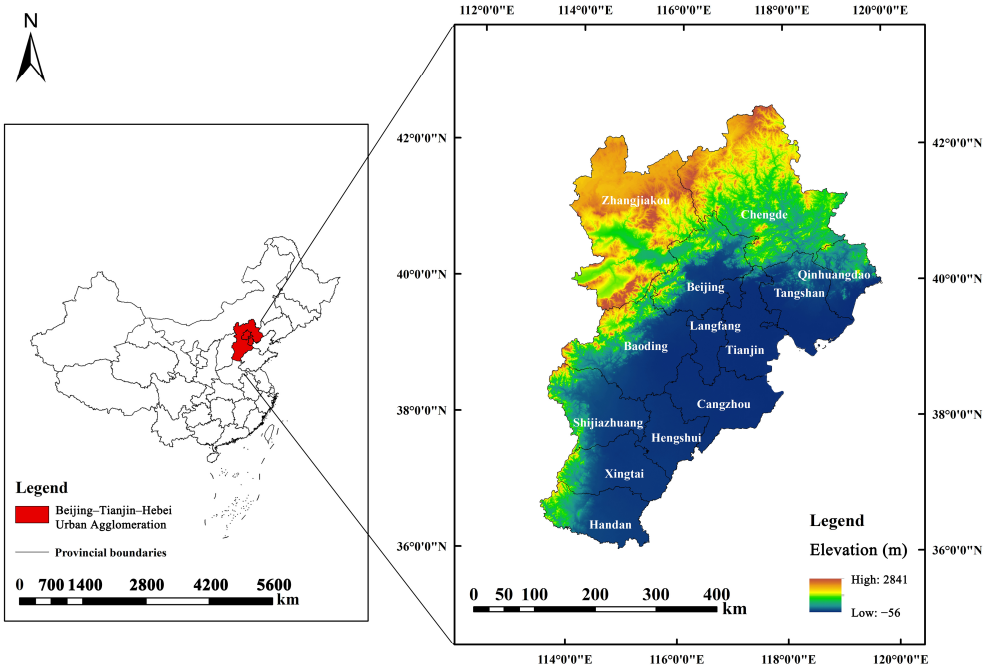


Figure 1. Overview of the study area.

2.2. Data Source and Pre-Processing

Land use data in the study area from 2000 to 2020 were derived from China Multi-Period Remote Sensing Land Use Monitoring Dataset (CNLUCC) [30], which was produced by the Institute of Geomatics Science and Natural Resources Research, Chinese Academy of Sciences, with a resolution of 30 m (http://www.resdc.cn (accessed on 10 April 2024)). This dataset is obtained by a manual visual interpretation based on Landsat remote sensing image data. It is available on an annual basis and includes land use data for 10 years: 1980, 1990, 1995, 2000, 2005, 2010, 2013, 2015, 2018 and 2020. In this study, we used the land use data from CNLUCC in 2000, 2010 and 2020 to quantify the dynamic land use changes and urban carbon metabolism. Using Arcgis 10.8 and the administrative boundaries, eight land

use types were obtained from the CNLUCC in the BTHUA: cropland, urban settlement, rural settlement, industrial and transportation land, barren land, forest land, grassland, and water bodies. The statistical data, including the population, energy consumption metrics, vehicle ownership statistics, livestock information, crop cultivation area data, agricultural economic indicators, crop yield data, port throughput figures, traffic volume data, and industrial energy usage statistics, were obtained from the Beijing Statistical Yearbook [31–33], Tianjin Statistical Yearbook [34–36], and Hebei Statistical Yearbook [37–39] in 2000, 2010, and 2020.

A flowchart illustrating the methodology is provided below (Figure 2). This flowchart summarizes the key steps taken in the study, including data collection, land use classification, carbon sequestration and emission calculations, and ecological network analysis.

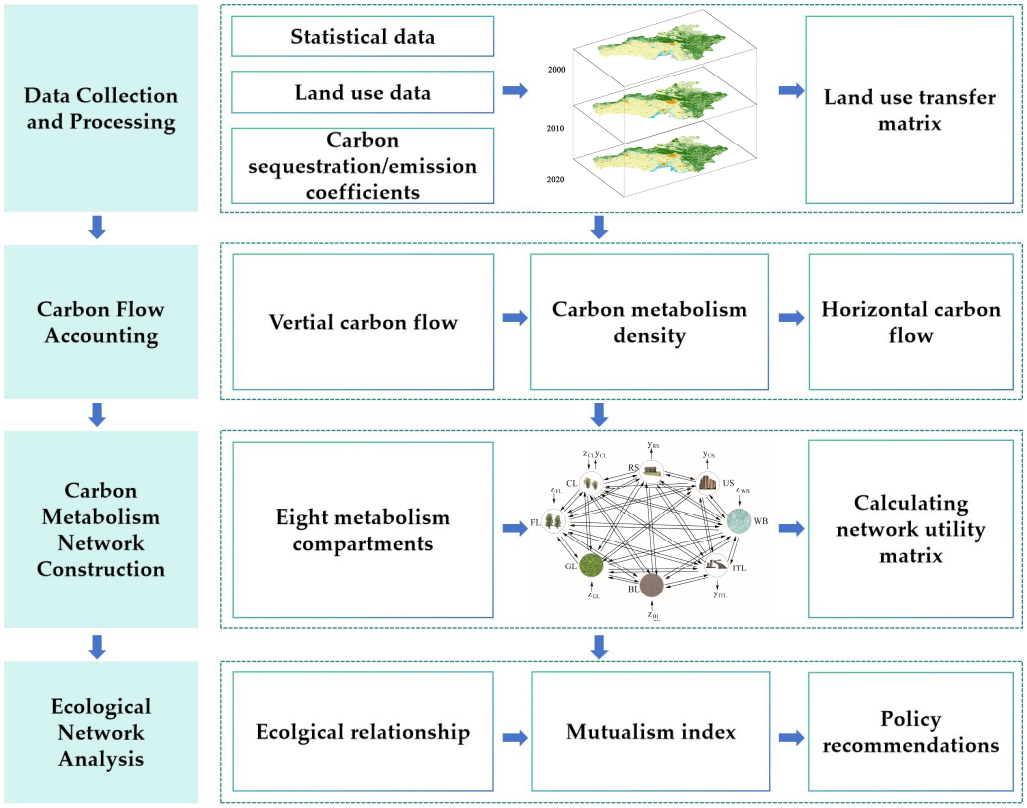


Figure 2. Methodology framework.

2.3. Accounting of Carbon Sequestration and Emissions

2.3.1. Carbon Sequestration

The carbon sequestration coefficient method assigns specific coefficients to each land use type, reflective of their inherent capacity to act in carbon sequestration. According to previous research [40–44], we utilized the carbon sequestration coefficients to estimate the carbon sequestration potential of cropland, forest land, grassland, water bodies, and barren land (Table 1). The calculation formula is as follows:

$$V_S = \sum kS \quad (1)$$

where S denotes the land use area, while k signifies the rate at which a unit area of land use type can sequester carbon (Table 1).

Table 1. The carbon sequestration coefficients for the land use types.

Land Use Type	Sub-Type	Carbon Sequestration Coefficient ($kg \cdot m^{-2} \cdot a^{-1}$)
Cropland	Cropland	0.0007
Forest land	Closed forest land	0.087
	Shrubland	0.023
	Sparse woodland	0.058
	Other forest	0.02327
Grassland	High-coverage grassland	0.0138
	Medium-coverage grassland	0.0046
	Low-coverage grassland	0.0021
Water bodies	River	0.0671
	Lake	0.0390
	Reservoir	0.0303
	Floodplain	0.00567
Barren land	Barren land	0.00005

2.3.2. Carbon Emissions

Utilizing the greenhouse gas inventory method developed by the Intergovernmental Panel on Climate Change (IPCC), we estimated carbon emissions associated with land uses, including cropland, industrial and transportation land, urban settlement, and rural settlement. In accordance with the 2019 Refinement of the 2006 IPCC Guidelines for National Greenhouse Gas Inventories [45] and the Guidelines for Provincial Greenhouse Gas Inventory Compilation in China, we identified carbon emission activities pertinent to each land use type (Table 2).

Table 2. Land use types and carbon emission activities.

Land Use Type	Carbon Emission Source
Cropland	Agricultural activities, livestock metabolism, and crop respiration
Industrial land	Industrial production, i.e., mining and manufacturing, and postal and telecommunications
Transportation land	Land transportation (i.e., private and public transport) and water transportation
Urban settlement	Urban living consumption and human respiration
Rural settlement	Rural human respiration, straw burning, and coal burning

(1) Carbon emissions from cropland

$$V_c = K_2M + K_3S_i + K_4D + K_5F + \sum K_cR_c + \sum K_jR_j \quad (2)$$

where V_c refers to carbon emissions from cropland; M is the amount of agricultural machinery; S_i represents the irrigated area; D is agricultural diesel consumption; F is the amount of applied fertilizer; and R_c refers to the annual yield. R_j is the number of livestock (pigs, cattle, and sheep in the BTHUA) raised over the year. Livestock's carbon emissions primarily consist of those produced by respiration and excretion. The carbon emission coefficients for cropland were derived from previous studies [6,9,46,47] and the statistical yearbook (Table 3).

Table 3. Carbon emission coefficients for cropland.

Code	Carbon Emission Activity	Carbon Emission Coefficient
K_2	Agricultural machinery	0.18 kgC·kW^{-1}
K_3	Irrigation	266.48 kgC·hm^{-2}
K_4	Agricultural diesel	0.5927 kgC·kg^{-1}
K_5	Used fertilizer	0.8956 kgC·kg^{-1}
K_6	Pig respiration	821.25 tC·10^{-4} head^{-1}
K_7	Pig excretion	31.35 tC·10^{-4} head^{-1}
K_8	Cattle respiration	7963.64 tC·10^{-4} head^{-1}
K_9	Cattle excretion	24.08 tC·10^{-4} head^{-1}
K_{10}	Sheep respiration	647.05 tC·10^{-4} head^{-1}
K_{11}	Sheep excretion	3.75 tC·10^{-4} head^{-1}
K_{12}	Carbon footprint of wheat area	2248 kgC·hm^{-2}
K_{13}	Carbon footprint of maize area	1446 kgC·hm^{-2}
K_{14}	Carbon footprint of wheat yield	0.476 kgC·kg^{-1}
K_{15}	Carbon footprint of maize yield	0.252 kgC·kg^{-1}

(2) Carbon emissions from industrial land

$$V_i = \sum E_i f_i \quad (3)$$

where V_i denotes carbon emissions from the industrial land, and E_i is the total industrial energy consumption. Following the IPCC method [15], energy consumption is equated to the standard coal amount multiplied by the corresponding carbon emission coefficient f_i (Table 4). The conversion factors were obtained from "General Principles for Calculation of the Comprehensive Energy Consumption GB/T2589-2008", which defines 1 kg of standard coal (1 kgce) as fuel with a low calorific value of 29,307 kJ.

Table 4. Carbon emission coefficients for the fuel types.

Fuel Type	Conversion Coefficient of Standard Coal (kgce·kg^{-1})	Carbon Emission Coefficient (kg·kgce^{-1})
Coal	0.7143	0.7559
Coke	0.9714	0.8550
Crude oil	1.4286	0.5857
Gasoline	1.4714	0.5538
Kerosene	1.4714	0.5714
Diesel	1.4571	0.5921
Fuel oil	1.4286	0.6185
Other petroleum products	1.2280	0.5857
Natural gas	1.2143	0.4483
Liquefied petroleum gas	1.7143	0.5042
Standard coal	1	0.67

(3) Carbon emissions from transportation land

$$V_T = V_1 + V_2 + V_W = K_{16}M_p + K_{17}M_B + K_{18}M_T + K_{19}M_M + T_iF_i + T_WF_3 \quad (4)$$

where V_T refers to carbon emissions from transportation land; V_1 is carbon emissions from travel traffic such as private cars, buses, taxis, and motorcycles; V_2 is carbon emissions from passenger and cargo transport, including road and rail transport; V_W is carbon emissions from inland river transportation; M_p, M_B, M_T, and M_M represent the average operating kilometers per year for private cars, buses, taxis, and motorcycles (i.e., 15,000 km, 60,000 km, 120,000 km and 4000 km, respectively). T_i represents the traffic volume of the ith type of passenger and cargo transportation; F_i

is the carbon emission coefficient for transportation type i (Table 5). T_W refers to the outgoing port throughput.

Table 5. Carbon emission coefficients for transportation.

Code	Transportation Type	Carbon Emission Coefficient
K_{16}	Private car	22.3 $kgC \cdot 10^{-2}\ km^{-1}$
K_{17}	Bus	88.1 $kgC \cdot 10^{-2}\ km^{-1}$
K_{18}	Taxi	28.3 $kgC \cdot 10^{-2}\ km^{-1}$
K_{19}	Motorcycle	6.7 $kgC \cdot 10^{-2}\ km^{-1}$
F_1	Passenger and freight transport on highways	0.02484 $kgC \cdot t^{-1} \cdot km^{-1}$
F_2	Passenger and freight transport on railways	0.0217 $kgC \cdot t^{-1} \cdot km^{-1}$
F_3	Passenger and freight transport on rivers	5.6 $tC \cdot 10^{-4} \cdot t^{-1}$

(4) Carbon emissions from urban settlement

$$V_u = \sum E_u f_i + K_1 P \quad (5)$$

where V_u represents the carbon emissions from urban settlement; E_u denotes residential energy consumption in terms of standard coal; f_i is the carbon emission coefficient for the fuel type (Table 4); K_1 is the carbon emission coefficient for human respiration, standardized at 79 $kg \cdot person^{-1} \cdot a^{-1}$; and P refers to the urban non-agricultural population.

(5) Carbon emissions from rural settlement

$$V_r = \sum R_c S_c f_i ab + K_1 P_r \quad (6)$$

where V_r represents the carbon emissions from rural settlement, which include straw burning and human respiratory carbon emissions; R_c is the crop yield; S_c is the ratio of grain to straw; f_i is the carbon emission coefficient for straw burning (Table 6); a and b are the straw open-air burning ratio and combustion efficiency, with values of 0.165 and 0.8, respectively [9].

Table 6. The grain-to-grass ratio and carbon emission coefficient for straw burning.

Crop Type	Ratio of Grain to Straw	Carbon Emission Coefficient for Straw Burning ($kgC \cdot kg^{-1}$)
Wheat	1.1	0.089
Maize	2	0.041

2.4. Carbon Flow Accounting

In this study, we constructed the carbon metabolism network based on the land use transfer matrix to quantify the carbon flow between different land use types (Figure 3). The carbon flow is categorized into two distinct directions: vertical and horizontal carbon flows. This separation is essential for understanding the different mechanisms through which carbon is exchanged within the urban ecosystem. Vertical carbon flow refers to the net carbon exchange within each land use type, calculated by subtracting the carbon emissions from the carbon sequestration values. A positive vertical carbon flow indicates that a land use type is acting as a carbon sink, sequestering more carbon than it emits, while a negative value signifies that it is a carbon source, emitting more carbon than it sequesters. This distinction is crucial for assessing the overall carbon balance of each land use type and understanding its role in urban carbon metabolism. Horizontal carbon flow, on the other hand, represents the transfer of carbon between different land use types. This flow occurs when land use changes result in the conversion of one type of land use to another, affecting the carbon dynamics of both the source and the destination land use types. By analyzing horizontal carbon flows, we can identify how land use changes impact the carbon

metabolism of the entire urban ecosystem, revealing the interconnectedness of different land uses and their collective influence on carbon emissions and sequestration. Each land use type represents a different compartment, and horizontal carbon flow (f_{ij}) is usually carried out between the compartments. Z represents carbon flow into a compartment from the outside (carbon sequestration), and Y represents carbon flow from a compartment to the outside (carbon emission). Forest land, grassland, barren land, and water bodies are usually regarded as carbon sequestration compartments, while rural settlement, urban settlement, and industrial and transportation land are considered carbon emission compartments.

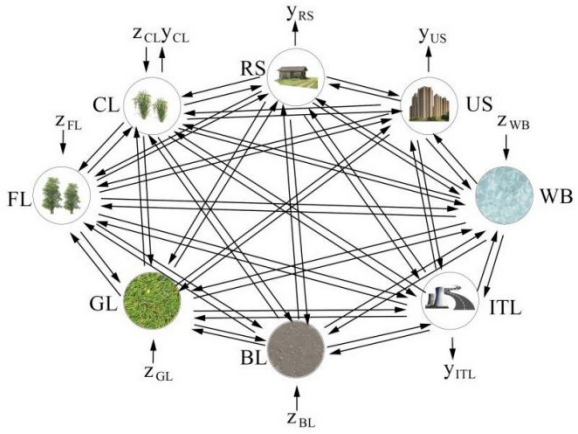


Figure 3. Carbon flow within and between the compartments (CL: cropland, US: urban settlement, ITL: industrial and transportation land, RS: rural settlement, FL: forest land, GL: grassland, WB: water body, BL: barren land).

In order to quantify carbon metabolism, we defined carbon emissions or carbon sequestration per unit area of each land use type as the carbon metabolism density. The formulas are listed below [48].

$$f_{ij} = \Delta W \cdot \Delta S \tag{7}$$

$$\Delta W = W_i - W_j = \frac{V_i}{S_i} - \frac{V_j}{S_j} \tag{8}$$

where i and j represent the compartments (i.e., land uses); W_i and W_j, V_i and V_j, and S_i and S_j refer to the net horizontal carbon flow densities, the net carbon flows, and the area of i and j, respectively; f_{ij} indicates the horizontal carbon flow from j to i; ΔW refers to the carbon metabolism density; and ΔS is the land use transfer area. If $\Delta W > 0$, it indicates an increase in carbon sequestration or a decrease in carbon emissions, suggesting a beneficial process for the balance of carbon metabolism.

2.5. Determination of Ecological Relationships

In this study, we employed ENA to quantify the ecological relationships between different land use types in the BTHUA. The analysis involved several statistical methods to assess the flow of carbon and the interactions between compartments.

To determine the ecological relationships, we first constructed a direct utility intensity matrix (D) that reflects the net carbon flow between compartments. This matrix captures the effective utilization rate of carbon metabolism activities between different land use types. The integral utility intensity matrix (U) was then derived from D, which encapsulates both the direct and indirect effects of interactions within the ecological network [22,49], the calculation formula is as follows:

$$d_{ij} = \frac{(f_{ij} - f_{ji})}{T_i} \tag{9}$$

$$D_{ij} = \begin{bmatrix} \left(\frac{(f_{jj}-f_{jj})}{T_j}\right) & \left(\frac{(f_{ji}-f_{ij})}{T_j}\right) \\ \left(\frac{(f_{ij}-f_{ji})}{T_i}\right) & \left(\frac{(f_{ii}-f_{ii})}{T_i}\right) \end{bmatrix} \quad (10)$$

$$U = (u_{ij}) = (I - D)^{-1} \quad (11)$$

where d_{ij} represents the net flow utility from j to i, reflecting the effective utilization rate of carbon metabolism activities between i and j; d is an element of matrix D, indicating the direct impact of each carbon flow path; and I is the identity matrix, representing the self-feedback from the flow rate of each compartment. U captures the ecological relationship between compartments through the positive and negative values of its elements, which represent the direct and indirect effects of interactions within the ecological network.

The analysis included various agricultural economic indicators that are crucial for understanding the dynamics of carbon emissions and sequestration in the BTHUA. These indicators include crop yield data, livestock information, energy consumption metrics, and agricultural economic indicators [50]. These indicators are crucial for understanding the carbon sequestration and emission dynamics within the agricultural sector, which are significant components of the urban carbon metabolism system [18].

The ecological relationships were quantified using the balance variable x_k introduced by Finn [51], where positive balance variables indicate an increase in system energy (i.e., carbon sequestration) and negative balance variables indicate a decrease (i.e., carbon emissions):

$$x_i = f_{in} - f_{out} \quad (12)$$

$$f_{in} = \sum f_{ki} \quad (13)$$

$$f_{out} = \sum f_{ij} \quad (14)$$

where x_i is defined as the change in carbon storage in compartment i; f_{in} and f_{out} represent the horizontal carbon flow into compartment i and out of compartment i, respectively; and f_{ki} and f_{ij} refer to the horizontal carbon flow from i to k and from j to i, respectively. If $x_i > 0$, it indicates an increase in carbon sequestration or a decrease in carbon emissions.

The mutualism index (M) denoted by Z was calculated to reflect the balance of positive to negative interactions within the matrix U. A mutualism index greater than 1 ($M > 1$) suggests that land use changes exert a positive influence on carbon metabolism, indicating a beneficial ecological relationship [52].

$$Z = \frac{Y^+}{Y^-} \quad (15)$$

where Y+ signifies the count of elements with a positive sign, while Y− denotes the count of those with a negative sign. A mutualism index (M) greater than 1 ($Z > 1$) suggests that the dynamic changes in land use types exert a positive influence on carbon metabolism. A higher value indicates a more pronounced beneficial effect.

The symbolic matrix (Table 7) was defined to categorize the relationships between compartments into four types: mutualism (+, +), competition (−, −), predation (+, −), and restriction (−, +). This classification allows for a nuanced understanding of how different land uses interact and influence carbon flows within the urban ecosystem [25].

Table 7. The ecological relationships between the compartments.

Matrix Notation	Positive +	Neutral 0	Negative −
Positive (+)	(+, +) mutualism	(+, 0) commensalism	(+, −) predation
Neutral (0)	(0, +) commensalism host	(0, 0) neutralism	(0, −) amensalism
Negative (−)	(−, +) restriction	(−, 0) amensal host	(−, −) competition

3. Results

3.1. Carbon Sequestration and Emission Changes

3.1.1. Land Use Changes from 2000 to 2020

The land use distribution in the BTHUA from 2000 to 2020 (Figure 4) shows that cropland was primarily located in the southeastern plain, whereas forest and grassland were predominantly situated in the mountainous area in the northwest. The urban area constituted the primary carbon-emitting zones. The rural settlement was dispersed and encircled by cropland.

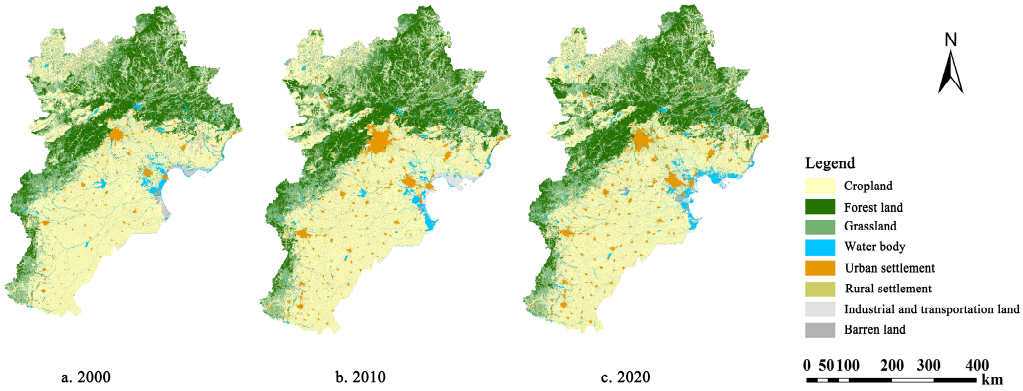


Figure 4. Land use map of the BTHUA from 2000 to 2020.

Cropland encompassed the largest portion of area, followed by forest land, grassland, and rural settlement, while water bodies, urban settlement, industrial and transportation land, and barren land accounted for comparatively smaller areas (Table 8). The area of cropland experienced a notable reduction from 2000 to 2020, with an overall decrease of 8.6%. In contrast, the areas of forest land, industrial and transportation land, and rural settlement increased consistently. Concurrently, urban settlement expanded from 2000 to 2010, surpassing twice its original area, followed by a slight decline. The area of water bodies diminished from 2000 to 2010, and then increased. The areas of forest land and grassland remained relatively stable over the study period.

Table 8. Land use area in the BTHUA from 2000 to 2020.

Land Use Type	Area (km^2)			Change Rate (%)		
	2000	2010	2020	2000–2010	2010–2010	2000–2020
Cropland	111,527.9	106,139.6	101,932.6	−4.8	−4.0	−8.6
Forest land	44,826.3	45,144.9	45,673.3	0.7	1.2	1.9
Grassland	35,815	34,556.7	34,554.1	−3.5	0.0	−3.5
Water body	6523.6	5774.1	7212.6	−11.5	24.9	10.6
Urban settlement	3658.2	7873.3	7219.9	115.2	−8.2	97.4
Rural settlement	12,251.4	14,773.5	16,576.8	20.6	12.2	35.3
Industrial and transportation land	2424	4114.9	4967.2	69.8	20.7	104.9
Barren land	2081.2	1290.8	1679.3	−38.0	30.1	−19.3

3.1.2. Carbon Sequestration Changes

Among the land use types, forest land had the highest carbon sequestration values, which was followed by grassland, water bodies, and cropland (Table 9). The carbon sequestration values of forest land showed a continuous increase of 7.1% from 2000 to 2020. Grassland demonstrated a relatively stable carbon sequestration potential with a slight decrease. The carbon sequestration of water bodies increased by 37.6%. Despite the dominance in land use, the carbon sequestration of cropland continued to decrease during the study period.

Table 9. Carbon sequestration values of the land use types from 2000 to 2020.

Land Use Type	Sub-Type	Carbon Sequestration (10^4 t)			Change Rate (%)		
		2000	2010	2020	2000–2010	2010–2020	2000–2020
Cropland		7.7	7.3	6.9	−4.8	−5.5	−10.4
Forest land		256.0	266.2	274.3	3.9	3.0	7.1
	Closed forest land	192.6	205.2	214.5	6.5	4.5	11.4
	Shrub land	41.0	39.2	38.1	−4.4	−2.8	−7.0
	Sparse woodland	19.4	19.7	19.7	1.5	−0.2	1.5
	Other forest	3.1	2.2	2.1	−29.0	−4.5	−32.2
Grassland		36.6	35.8	35.9	−2.2	0.3	−1.9
	High-coverage grassland	31.3	30.9	31.1	−1.3	0.6	−0.6
	High-coverage grassland	4.9	4.5	4.5	−8.2	−1.5	−8.2
	Low-coverage grassland	0.4	0.4	0.4	−14.0	1.5	−12.5
Water bodies		18.6	20.5	25.6	10.2	25.1	37.6
	River	9.2	12.0	12.3	30.4	2.5	33.7
	Lake	0.8	0.7	1.2	−12.5	71.4	50
	Reservoir	7.2	6.9	11.5	−4.2	66.7	59.7
	Floodplain	14.5	0.9	0.7	−93.8	−22.2	−95.2
Barren land		0.0	0.0	0.0	−38.0	30.0	−19.3

In the study, we utilized Natural Breaks (Jenks) method in ArcGIS 10.8, which could automatically classify the accounting results and reduce the intra-class variance and maximize the inter-class variance, to classify the carbon sequestration density, carbon emission density, and vertical carbon flow density into five classes. The values of carbon sequestration density were categorized into five categories: low (0~6.8 t·km^{-2}), relatively low (6.81~13.6 t·km^{-2}), medium (13.61~20.4 t·km^{-2}), relatively high (20.41~27.2 t·km^{-2}), and high (27.21~34 t·km^{-2}) (Figure 5). The carbon sequestration density of most cities remained stable. Cities in the northern part, which are rich in forest and grassland resources, showed higher carbon sequestration densities than those in the southeast that are primarily composed of cropland. For example, the highest carbon sequestration density in Chengde indicated the substantial contributions of forest and grassland.

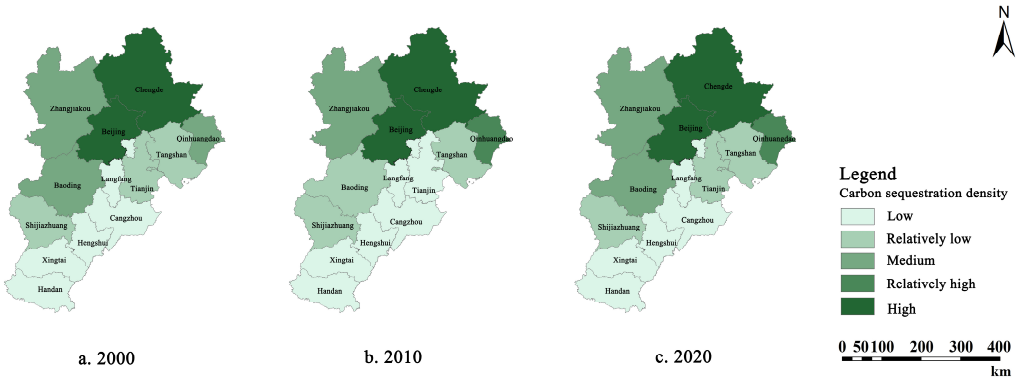


Figure 5. Carbon sequestration density from 2000 to 2020.

In general, the average carbon sequestration density in the BTHUA increased from 2000 to 2020. The areas of Chengde and Beijing with highest carbon sequestration densities covered 24.9% of the total area in this region. Qinghuangdao was the only city with relatively high carbon sequestration densities in 2010 and 2020. Baoding and Tianjin experienced a decrease in the carbon sequestration density, followed by an increase. Six cities, including Langfang, Cangzhou, Hengshui, Xingtai and Handan, remained at low carbon sequestration densities during the study period.

3.1.3. Carbon Emission Changes

The carbon emissions from the land use types (Table 10) show that the industrial and transportation land had the highest carbon emissions during the study period, which was followed by the cropland and urban settlement. Besides that, the industrial and transportation land and urban settlement depicted high increasing rates (165.3% and 200.7%) from 2000 to 2020. The carbon emission values of the rural settlement increased continuously. Only the carbon emissions from the cropland decreased by 11.1% from 2010 to 2020. The total carbon emissions increased by 145.3% during the study period.

Table 10. Carbon emissions from the land use types from 2000 to 2020.

Land Use Type	Carbon Emission (10^4 t)			Change Rate (%)		
	2000	2010	2020	2000–2010	2010–2020	2000–2020
Cropland	2336.8	2381.5	2116.7	1.9	−11.1	−9.4
Industrial and transportation land	14,418.6	26,102.7	38,258.4	81.0	46.6	165.3
Rural settlement	386.7	499.5	600.76	29.2	20.3	55.3
Urban settlement	1948.7	3327.5	5858.9	70.8	76.1	200.7

The carbon emission density was calculated by dividing the total carbon emissions by the administrative area. The values were classified into five levels based on the Natural Breaks (Jenks) method: low (0~1.6 × 10^3 t·km^{-2}), relatively low (1.61 × 10^3~3.2 × 10^3 t·km^{-2}), medium (3.21 × 10^3~4.8 × 10^3 t·km^{-2}), relatively high (4.81 × 10^3~6.4 × 10^3 t·km^{-2}), and high (6.41 × 10^3~8 × 10^3 t·km^{-2}) (Figure 6). The result indicated an increasing trend for the average values of carbon emission density from 2000 to 2020. Among all the cities in in the BTHUA, Tangshan and Tianjin had the highest carbon emission densities. Four cities, including Chengde, Zhangjiakou, and Hengshui, remained at low values. Baoding, Shijiazhuang, Handan, Cangzhou, Langfang, Beijing, and Qinghuangdao experienced an obvious increase in the carbon emission densities from 2010 to 2020.

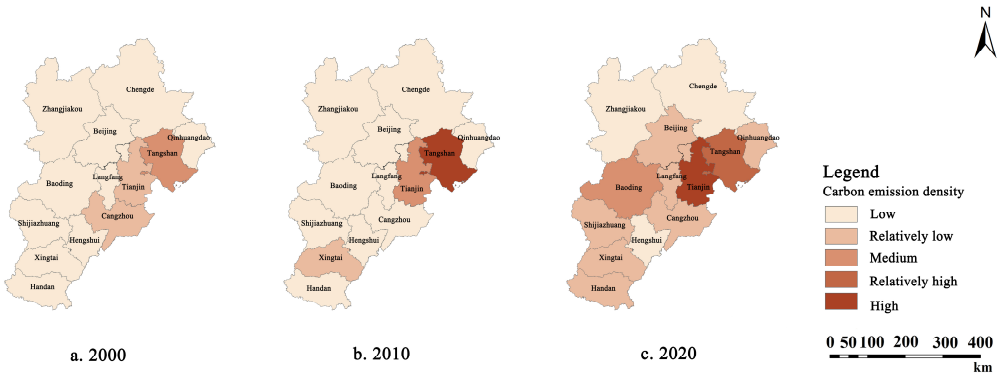


Figure 6. Carbon emission density from 2000 to 2020.

3.2. Vertical Carbon Flow Changes

A positive vertical carbon flow value means that the carbon sequestration value is higher than the carbon emission value (Table 11). The negative vertical carbon flows show that cropland, urban settlement, industrial and transportation land, and rural settlement function as carbon sources in the BTHUA, while forest land, grassland, and water bodies are recognized as net carbon sequestration pools in the study area. The urban settlement, industrial and transportation land, and rural settlement experienced a continuous increase in the absolute values of vertical carbon flow from 2000 to 2020. Industrial land emerged as a critical carbon source in the BTHUA, which was followed by the cropland, urban settlement, transportation land, and rural settlement. The positive vertical carbon flows of forest land kept increasing during the study period, while the values of grassland and

water bodies experienced a decrease from 2000 to 2010, which was followed by an increase in the second period.

Table 11. Vertical carbon flows for the land use types from 2000 to 2020.

Land Use Type	Vertical Carbon Flow (10^4 t)			Change Rate of the Absolute Vertical Carbon Flow Value (%)		
	2000	2010	2020	2000–2010	2010–2020	2000–2020
Cropland	−2329.1	−2374.2	−2109.8	1.9	−11.1	−9.4
Forest land	256	266.2	274.3	4.0	3.0	7.1
Grassland	36.6	35.8	35.9	−2.2	0.3	−1.9
Water bodies	18.6	20.5	25.6	10.2	25.1	37.6
Urban settlement	−1948.7	−3327.5	−5858.9	70.8	76.1	200.7
Industrial land	−12,359.6	−18,520.1	−22,914.1	49.8	23.7	85.4
Transportation land	−2058.9	−7582.6	−15,344.3	268.3	102.3	645.3
Rural settlement	−386.7	−499.5	−600.76	29.1	20.3	55.4
Barren land	0.0	0.0	0.0	−38.0	30.0	−19.3

The vertical carbon flow density was calculated by dividing the vertical carbon flow by the area. The values were classified into five levels based on the Natural Breaks (Jenks) method: low (-8×10^3~-6.41×10^3 t·km^{-2}), relatively low (-6.4×10^3~-4.81×10^3 t·km^{-2}), medium (-4.8×10^3~-3.21×10^3 t·km^{-2}), relatively high (-3.2×10^3~-1.61×10^3 t·km^{-2}), and high (-1.6 ~0 $\times 10^3$ t·km^{-2}) (Figure 7). The negative vertical carbon flow density values indicated a comprehensive manifestation of carbon emissions in the BTHUA. Tianjin and Tangshan have been identified as cities with the lowest vertical carbon flow densities. The vertical carbon flow densities in Zhangjiakou, Chengde, and Hengshui remained stable and high throughout the study period. Eight cities, including Tianjin, Beijing, Baoding, Xintang, Handan, Shijiazhuang, Qinghuangdao, and Langfang, experienced a decrease in vertical carbon flow densities.

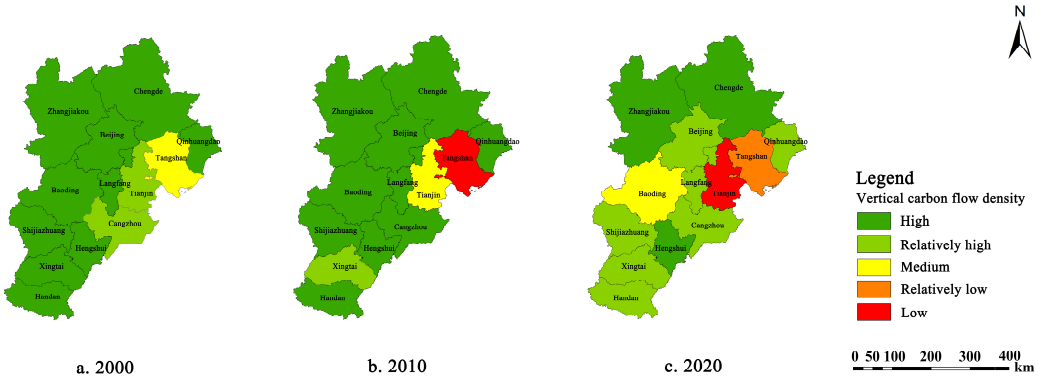


Figure 7. Vertical carbon flow density from 2000 to 2020.

3.3. Horizontal Carbon Flow Changes

3.3.1. Carbon Metabolism Density

The land use transfer for the entire study period revealed that the area of cropland the transformed into other types remained the most substantial (Figure 8), which was followed by the transfer from grassland to other land uses. Cropland was mainly shifted to rural settlement. Grassland was converted to forest land and cropland. The smallest area of transfer was attributed to urban settlement, indicating the relatively effective control over urban expansion. A notable decline in land use transfer activity was observed from 2010 to 2000 compared to the first period.

The change in the net horizontal carbon flow density for eight land uses (Table 12) showed that industrial and transportation land, urban settlement, cropland, and rural settlement were identified as negative carbon metabolism compartments, whereas barren land, forest land, grassland, and water bodies were classified as positive carbon metabolism compartments. The land use transfer from the positive carbon metabolism compartments to

other compartments experienced a reduction during the study period, yet the predominant conversion was from these compartments into cropland. In contrast, the area of negative carbon metabolism compartments that transformed into forest land, grassland, and water bodies showed a substantial increase, with the most considerable shift being from industrial and transportation land into water bodies.

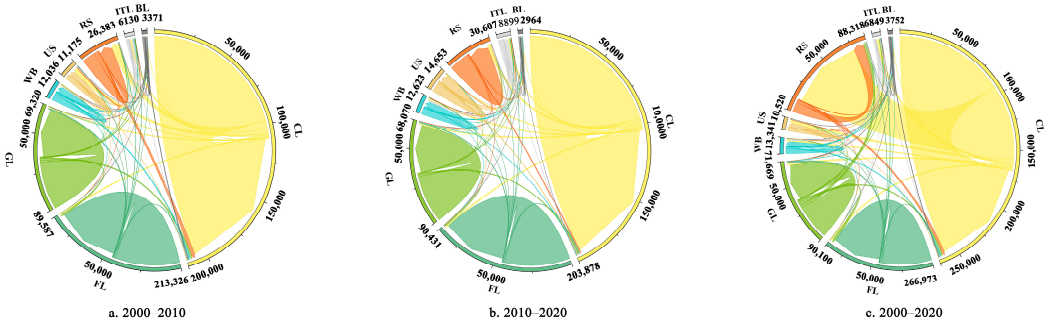


Figure 8. Land use transfer from 2000 to 2020 (km^2) (CL: cropland, US: urban settlement, ITL: industrial and transportation land, RS: rural settlement, FL: forest land, GL: grassland, WB: water body, BL: barren land).

Table 12. Net horizontal carbon flow density of the land use types from 2000 to 2020.

Land Use Type	Net Horizontal Carbon Flow Density ($t \cdot km^{-2}$)		
	2000	2010	2020
Cropland	−203.8	−218.0	−201.6
Forest land	56.8	58.6	59.7
Grassland	10.1	10.2	10.3
Water bodies	28.4	35.3	35.4
Urban settlement	−5287.44	−4202.8	−8034.7
Industrial and transportation land	−59,463.54	−63,266.3	−76,679.0
Rural settlement	−306.1	−329.5	−354.1
Barren land	0.05	0.05	0.05

Industrial and transportation land exhibited the most substantial negative net horizontal carbon flow density, indicating its dominant role in carbon emissions. The conversion of other land uses to urban settlement and industrial and transportation land resulted in negative horizontal carbon flows due to their high negative carbon metabolism effects. Among the compartments with a positive carbon metabolism effect, barren land showed a low net carbon horizontal flow density. In contrast, forest land, which was engaged in the most abundant and effective carbon sequestration activities, presented a high net carbon flow density, which was followed by water bodies and grassland.

The carbon metabolism density refers to the amount of carbon that is processed or metabolized within a specific volume or area (Table 13). A positive value indicates a beneficial impact on carbon sequestration, while a negative value suggests a detrimental effect. The conversion of other land uses to industrial and transportation land exhibited the most obvious negative carbon metabolism effect, which was followed by the transfer of other land uses to urban settlement. The negative carbon metabolism impact was stronger in the period from 2010 to 2020 than in the first period. The conversion of industrial and transportation land and urban settlement into forest land, water bodies and grassland resulted in more positive carbon metabolism.

Table 13. Carbon metabolism density from 2000 to 2010 (t·km^{-2}) *.

2000\2010	CL	FL	GL	WB	US	RS	ITL	BL
CL	−14.2	262.4	214.0	239.1	−3999.0	−125.8	−63,062.5	203.8
FL	−274.7	1.9	−46.5	−21.4	−4259.5	−386.3	−63,323.0	−56.7
GL	−228.1	48.5	0.1	25.2	−4212.9	−339.7	−63,276.4	−10.1
WB	−246.3	30.2	−18.1	−7.0	−4231.2	−359.7	−63,294.7	−28.3
US	5069.5	5346.0	5298.7	5322.8	1084.7	4957.9	−57,978.8	5287.5
RS	88.1	364.7	316.3	341.4	−3896.7	−23.5	−62,960.2	306.1
ITL	59,245.6	59,522.1	59,473.8	63,301.6	55,260.7	59,134.0	−3802.8	59,463.6
BL	−218.0	58.6	10.2	35.3	−4202.8	−329.6	−63,266.3	0.0
2010\2020	**CL**	**FL**	**GL**	**WB**	**US**	**RS**	**ITL**	**BL**
CL	16.8	277.7	228.2	253.3	−7816.7	−136.1	−76,461.1	218.0
FL	−260.2	1.1	−48.3	−23.3	−8093.3	−412.7	−76,737.6	−58.6
GL	−211.8	49.4	0.0	25.1	−8044.9	−364.3	−76,689.3	−10.2
WB	−236.9	24.3	−25.1	0.0	−8070.0	−389.4	−76,714.4	−35.3
US	4001.2	4262.5	4213.1	4238.1	−3831.9	3848.7	−72,476.2	4202.8
RS	128.0	389.2	339.8	364.9	−7705.1	−24.5	−76,349.5	329.6
ITL	63,064.7	63,326.0	63,276.6	63,301.6	55,231.6	62,912.2	−13,412.7	63,266.3
BL	−201.6	59.6	10.2	35.3	−76,679.1	−354.1	−76,679.1	0.0
2000\2020	**CL**	**FL**	**GL**	**WB**	**US**	**RS**	**ITL**	**BL**
CL	−2.2	263.5	214.0	239.1	−7830.9	−150.3	−76,475.3	203.8
FL	−258.3	2.9	−46.5	−21.4	−8091.4	−410.8	−76,735.8	−56.7
GL	−211.7	49.6	0.2	25.2	−8044.8	−364.2	−76,689.1	−10.1
WB	−229.9	31.3	−18.1	−7.0	−8063.0	−382.5	−76,707.4	−28.3
US	5085.9	5347.1	5297.7	5322.8	−2747.2	4933.4	−71,391.6	5287.5
RS	104.5	365.7	316.3	341.4	−7728.6	−48.0	−76,373.0	306.1
ITL	59,262.0	59,523.2	59,473.8	59,498.9	51,428.9	59,109.4	−17,215.5	59,463.6
BL	−201.6	59.6	10.2	35.3	−8034.7	−354.1	−76,679.1	0.0

* CL: cropland, US: urban settlement, ITL: industrial and transportation land, RS: rural settlement, FL: forest land, GL: grassland, WB: water body, BL: barren land.

3.3.2. Horizontal Carbon Flow

Horizontal carbon flow (Table 14) was calculated based on the carbon metabolism density and land use transfer in the BTHUA. The net horizontal carbon flow during the whole study period was negative, which indicated the negative impact of land use changes on the balance of carbon metabolism.

Negative horizontal carbon flow occurs when a land use type transferred to another with a lower carbon sequestration capacity. During the study period, the primary source of the negative horizontal carbon flow was the conversion of cropland to industrial and transportation land, constituting nearly half of the total negative horizontal carbon flow. The conversion of other land uses to industrial and transportation land and urban settlement also contributed to the increase in negative horizontal carbon flow.

On the one hand, the negative horizontal carbon flow that resulted from the conversion of forest land, grassland, and water bodies into industrial and transportation land, as well as the transformation of cropland into urban settlement, decreased in the second period (2010–2020) compared to the first period. On the other hand, the negative horizontal carbon flow caused by the conversion of urban and rural settlements to industrial and transportation land increased from 2010 to 2020, which highlighted that the industrial and transportation development in urban and rural settlements were significant contributors to increased carbon emissions.

The primary source of the positive horizontal carbon flow stemmed from the conversion of industrial and transportation land into water bodies, accounting for 53.5% and 61.3% of the positive horizontal carbon flow during the two periods, respectively. The transformation of industrial and transportation land into other land uses generated positive horizontal carbon flow. The positive horizontal carbon flow increased during the second period, reflecting a shift towards land use practices that enhanced the carbon sequestration potential.

Table 14. Horizontal carbon flow from 2000 to 2020 (10^4 tC) *.

Horizontal Carbon Flow	2000–2010	2010–2020	2000–2020
Negative horizontal carbon flow	−18,431.58	−20,155.51	−33,075.7
Positive horizontal carbon flow	6808.21	11,826.59	10,961.38
Net horizontal carbon flow	−11,687.1	−8328.92	−22,114.3
CL→FL	27.11	30.84	36.24
CL→GL	17.93	26.91	37.23
CL→WB	12.73	27.62	30.78
CL→US	−1116.16	−662.13	−2126.94
CL→RS	−63.73	−28.46	−96.49
CL→ITL	−8431.18	−9597.19	−17,380.70
CL→BL	1.13	3.79	2.41
FL→CL	−16.42	−22.57	−23.32
FL→GL	−4.76	−3.14	−7.44
FL→WB	−0.11	−0.27	−0.16
FL→US	−46.82	−16.42	−46.03
FL→RS	−8.47	−2.10	−8.17
FL→ITL	−1320.85	−1134.10	−2628.60
FL→BL	−0.03	−0.12	−0.08
GL→CL	−28.54	−17.43	−32.00
GL→FL	6.13	5.06	11.54
GL→WB	0.28	0.24	0.62
GL→US	−27.41	−15.32	−54.03
GL→RS	−7.83	−2.22	−9.55
GL→ITL	−2670.77	−2381.13	−5149.48
GL→BL	−0.24	−0.06	−0.19
WB→CL	−28.41	−8.58	−22.03
WB→FL	0.41	0.10	0.38
WB→GL	−0.15	−0.55	−0.54
WB→US	−88.70	−28.87	−135.14
WB→RS	−4.01	−2.19	−6.19
WB→ITL	−3230.91	−2252.20	−2337.92
WB→BL	−0.22	−1.52	−1.46
US→CL	47.88	177.29	39.65
US→FL	2.01	33.45	4.07
US→GL	2.25	50.82	9.21
US→WB	3.24	33.19	10.04
US→RS	26.46	328.24	−63.79
US→ITL	−95.80	−2045.33	−616.51
US→BL	0.0004	1.35	0.13
RS→CL	21.03	11.48	23.59
RS→FL	0.92	4.25	1.53
RS→GL	1.40	2.01	2.36
RS→WB	1.09	2.23	2.45
RS→US	−304.95	−145.20	−428.11
RS→ITL	−700.23	−1449.76	−1264.88
RS→BL	0.28	0.36	0.37
ITL→CL	125.89	1253.36	1017.22
ITL→FL	143.95	208.93	192.55
ITL→GL	167.83	628.45	429.94
ITL→WB	3644.73	7247.00	6545.71
ITL→US	1534.09	283.42	946.17
ITL→RS	999.92	1167.64	1435.68
ITL→BL	18.73	297.75	180.39
BL→CL	−13.97	−0.90	−12.51
BL→FL	0.31	0.04	0.31
BL→GL	0.33	0.07	0.32
BL→WB	0.15	0.7	0.49
BL→US	−13.37	−3.71	−23.23
BL→RS	−1.36	−0.17	−1.77
BL→ITL	−269.91	−333.87	−598.42

* CL: cropland, US: urban settlement, ITL: industrial and transportation land, RS: rural settlement, FL: forest land, GL: grassland, WB: water body, BL: barren land.

3.4. Ecological Relationships Between the Compartments

The values in the direct utility matrix D from 2000 to 2020 (Table 15) denoted the direct utilization rate of carbon flow, serving as a fundamental component for the integral utility matrix. A positive direct utilization rate indicates that the land use transfer positively

influences carbon metabolism, whereas a negative value suggests an adverse impact. From 2000 to 2010, the conversion of the cropland to urban settlement exhibited the most substantial negative direct utilization rate, indicating that this transition had the highest efficiency in generating negative horizontal carbon flow. Additionally, the transfer of rural settlement to urban settlement also demonstrated a relatively high negative direct utilization rate. For the positive values, the conversion of industrial and transportation land to urban settlement showed the highest direct utilization rate. The relatively high rates for the transfer of industrial and transportation land to other land uses further confirmed that the proper management of such land use can enhance sustainable carbon metabolism processes. However, the absolute values of the negative direct utilization rates decreased from 2010 to 2020. In general, the positive horizontal carbon flows were mainly provided through the transfer of industrial and transportation land to other land uses.

Table 15. The direct utility matrix D from 2000 to 2020 *.

2000\2010	**CL**	**FL**	**GL**	**WB**	**US**	**RS**	**ITL**	**BL**
CL	0	0.24	0.25	0.01	−83.3	−0.09	−1.24	0.77
FL	−0.04	0	−0.06	−0.0001	−3.50	−0.01	−0.18	−0.02
GL	−0.04	0.06	0	0.0001	−2.12	−0.01	−0.37	−0.03
WB	−0.03	0.002	−0.002	0	−6.58	−0.005	−0.88	−0.02
US	0.94	0.27	0.16	0.03	0	0.35	−0.21	0.68
RS	0.07	0.05	0.05	0.001	−21.54	0	−0.22	0.09
ITL	7.81	8.10	15.36	1.88	116.67	1.81	0	14.69
BL	−0.01	0.002	0.003	0.0001	−0.96	−0.002	−0.04	0
2010\2020	**CL**	**FL**	**GL**	**WB**	**US**	**RS**	**ITL**	**BL**
CL	0	0.19	0.06	0.005	1.43	−0.03	−0.97	0.02
FL	−0.04	0	−0.01	−0.0001	0.08	−0.004	−0.12	−0.0005
GL	−0.03	−0.08	0	0.0001	0.112	−0.003	−0.27	−0.0004
WB	−0.03	−0.10	−0.001	0	0.11	−0.003	−0.85	−0.007
US	0.60	0.18	0.09	0.008	0	0.32	−0.21	0.02
RS	0.03	0.02	0.006	0.0006	0.80	0	−0.24	0.002
ITL	7.79	4.57	4.27	1.30	−3.96	1.79	0	2.09
BL	−0.003	−0.01	0.0002	0.0003	0.009	−0.0004	−0.03	0
2000\2020	**CL**	**FL**	**GL**	**WB**	**US**	**RS**	**ITL**	**BL**
CL	0	0.24	0.15	0.008	4.42	−0.09	−3.33	0.08
FL	−0.06	0	−0.04	−0.0001	0.10	−0.007	−0.51	−0.002
GL	−0.07	0.08	0	0.0002	0.13	−0.009	−0.52	−0.000
WB	−0.05	0.002	−0.002	0	0.30	−0.006	−0.83	−0.01
US	2.19	0.20	0.13	0.02	0	0.36	−0.15	0.13
RS	0.12	0.04	0.03	0.001	1.00	0	−0.25	0.01
ITL	18.57	11.44	11.83	1.33	−3.19	1.96	0	4.29
BL	−0.02	0.002	0.001	0.0003	0.05	−0.002	−0.07	0

* CL: cropland, US: urban settlement, ITL: industrial and transportation land, RS: rural settlement, FL: forest land, GL: grassland, WB: water body, BL: barren land.

The integral utility matrix U from 2000 to 2020 revealed the ecological relationships between the compartments based on the positive or negative signs of the matrix elements (Table 15). According to the rules (Table 7), four typical ecological relationships were marked in colors (Table 16), that is, red means predation (+, −), blue stands for restriction (−, +), yellow refers to competition (−, −), and green represents mutualism (+, +).

Throughout the study period, predation and restriction predominantly characterized the ecological dynamic (Table 17). Predation was mainly observed in the industrial and transportation land and rural settlement, while restriction was evident in positive carbon metabolism compartments, such as forest land, grassland, and water bodies. Competition mainly occurred between urban settlement and other land uses, indicating that urban settlement's utility was compromised in its interactions with other land uses. Mutualism was observed in the transitions between urban settlement and industrial and transportation land throughout the study period and primarily within the positive carbon metabolism compartments from 2010 to 2020.

Table 16. Changes in the ecological relationships based on the integral utility matrix U from 2000 to 2020 *.

2000–2010	CL	FL	GL	WB	US	RS	ITL	BL
CL		−	−	−	−	+	+	−
FL	+		+	+	−	+	+	+
GL	+	−		−	−	+	+	+
WB	+	−	+		−	+	+	+
US	−	−	−	−		−	+	−
RS	−	−	−	−	−		+	−
ITL	−	−	−	−	+	−		−
BL	+	−	−	−	−	+	+	
2010–2020	**CL**	**FL**	**GL**	**WB**	**US**	**RS**	**ITL**	**BL**
CL		−	−	−	−	+	+	−
FL	+		+	+	−	+	+	+
GL	+	+		−	−	+	+	+
WB	+	+	+		−	+	+	+
US	−	−	−	−		−	+	−
RS	−	−	−	−	−		+	−
ITL	−	−	−	−	+	−		−
BL	+	+	−	−	−	+	+	
2000–2020	**CL**	**FL**	**GL**	**WB**	**US**	**RS**	**ITL**	**BL**
CL		−	−	−	−	+	+	−
FL	+		+	+	−	+	+	+
GL	+	−		−	−	+	+	+
WB	+	−	+		−	+	+	+
US	−	−	−	−		−	+	−
RS	−	−	−	−	−		+	−
ITL	−	−	−	−	+	−		−
BL	+	−	−	−	−	+	+	

* CL: cropland, US: urban settlement, ITL: industrial and transportation land, RS: rural settlement, FL: forest land, GL: grassland, WB: water body, BL: barren land.

Table 17. Ecological relationships between land use types from 2000 to 2020 *.

Ecological Relationship	CL	FL	GL	WB	US	RS	ITL	BL
Competition	3	3	3	3	18	3	0	3
Predation and Restriction	18	15	17	17	0	18	18	17
Mutualism	0	3	1	1	3	0	3	1

* CL: cropland, US: urban settlement, ITL: industrial and transportation land, RS: rural settlement, FL: forest land, GL: grassland, WB: water body, BL: barren land.

The spatial distribution of ecological relationships (Figure 9) showed that, from 2000 to 2010, the area with predation and restriction constituted 75% of the ecological relationships, primarily in the rural settlement and cropland in the southeastern part, as well as in patches or bands in the industrial and transportation land and ecological spaces on the eastern and western sides. From 2010 to 2020, the area with predation and restriction decreased to 64.3%, and the decrease was mainly observed in the northeast and southwest. These two relationships were concentrated in the central part, specifically along the Zhangjiakou–Beijing–Tianjin–Tangshan corridor and in the water bodies.

Competition, accounting for 21.43% of the ecological relationships, was mainly distributed in the urban area. From 2000 to 2010, competition was clustered at the edges of urban area in Beijing and Tianjin. Land use transfer led to competition for carbon storage between urban land use and other types. The spatial extent of the competitive relationship decreased from 2010 to 2020 and it showed a trend of outward expansion. The mutualism index (M) was 0.69 and 0.89 for the two periods. The values lower than one suggested a consistent negative impact of land use changes on the balance of carbon metabolism. The

increase in the M value from 2010 to 2020 indicated a less negative influence of land use alterations on carbon metabolism.

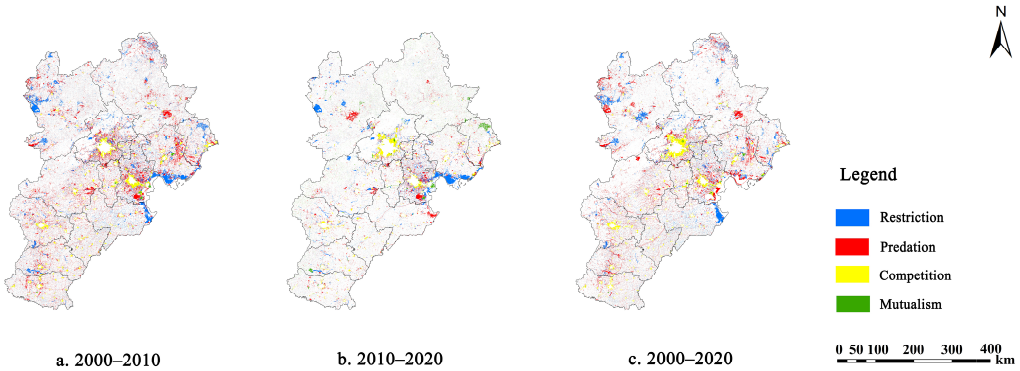


Figure 9. Spatial distribution of ecological relationships in the BTHUA.

4. Discussion

This study investigated the spatio-temporal dynamics of carbon metabolism in the BTHUA from 2000 to 2020, employing ENA to analyze the intricate relationships between land use changes and carbon flows. The findings reveal critical insights into the drivers of carbon emissions and sinks, offering valuable information for policy formulation and urban planning strategies aimed at mitigating climate change within the region.

4.1. Land Use Change and Policy Implementation

The BTHUA has undergone significant land use changes over the past two decades, driven by rapid urbanization and industrialization. These changes have had profound impacts on the region's carbon metabolism, as evidenced by our findings. The shift from natural landscapes to urban and industrial areas has increased carbon emissions, while reducing the region's carbon sequestration capacity. This aligns with national trends in China, where rapid economic growth and industrialization have historically prioritized development over environmental concerns. Previous studies also have highlighted the detrimental effects of urban expansion on carbon sinks [53,54].

Policy measures implemented during the study period have aimed to balance economic growth with environmental sustainability. For example, China's national policies, particularly the implementation of the 11th and 12th Five-Year Plans (2006–2010 and 2011–2015, respectively), emphasized energy efficiency and emissions reductions. These policies likely contributed to the observed slowdown in the growth rate of carbon emissions in the later years of the study period. Furthermore, the Beijing–Tianjin–Hebei Coordinated Development Plan initiated in 2014 specifically targeted environmental protection and ecological restoration [55]. This strategy promoted afforestation, ecological redline protection, and industrial restructuring, which are reflected in the increased carbon sequestration capacity of forest land and the improved mutualistic relationships within the carbon metabolism network [54]. The increase in forest coverage from 2000 to 2020 can be attributed to successful afforestation policies, including the "Green Belt" program and the "Million Mu Afforestation Project" [56]. These initiatives have enhanced the region's carbon sink capacity, as evidenced by our finding that forest land demonstrated the highest carbon sink density. However, our results indicate that these policies have not fully mitigated the negative impacts of land use changes on carbon metabolism. For example, the continued loss of cropland to urban development suggests a need to balance urbanization with agricultural land preservation [57]. The increase in industrial and transportation land, which exhibited the highest carbon emission density, suggests that economic priorities have often overshadowed environmental considerations. This finding underscores the need for more stringent policy measures that prioritize carbon reduction in urban planning and development [57].

The observed increase in the mutualism index (M) suggests some positive effects of policy interventions on carbon metabolism. This index reflects the degree of cooperation between different land use types in carbon exchange processes. The increase in M indicates a reduction in the negative impacts of LULC changes, possibly due to improved land management practices and the implementation of green infrastructure projects. However, the persistence of negative net horizontal carbon flows highlights the ongoing challenges in achieving sustainable urban development in the BTHUA [58].

4.2. ENA and Carbon Metabolism

The application of ENA in this study has provided valuable insights into the complex interactions between different land use types and their contributions to carbon metabolism. The results revealed that the ecological relationships in the BTHUA are predominantly characterized by restriction and predation, with competition mainly present in urban areas. This finding aligns with studies of other Chinese megacities [59] and urban agglomerations [60]. The competitive relationships observed mainly in urban areas reflect the intensive human activities and high energy consumption patterns characteristic of metropolitan regions. They underscore the need for more stringent land use regulations and stricter enforcement of environmental protection policies, particularly in rapidly urbanizing areas. The findings also highlight the importance of integrating carbon sequestration considerations into urban planning and land management practices [16]. The negative net horizontal carbon flow indicates that land use changes have disrupted the natural carbon balance, consistent with the findings from similar urban agglomerations [58]. This suggests that the conversion of land to urban and industrial uses still outpaces the gains from ecological restoration efforts.

However, the increasing mutualism index (M) suggests an improving trend in system stability, which is potentially attributed to better land use planning and environmental policies. The mutualism observed between positive carbon metabolism compartments, such as forest land and grassland, highlights the potential for spatial planning to transform ecological relationships and enhance carbon sequestration. This underscores the importance of integrating ecological considerations into urban planning processes to optimize carbon metabolism and mitigate climate change impacts [61]. The strategic placement of green infrastructure and the creation of ecological corridors can enhance carbon sequestration and promote synergistic interactions between different land use types [62]. This finding supports the growing body of literature advocating for nature-based solutions for urban carbon management [63].

Our study also highlights the utility of ENA in identifying key carbon sources and sinks within urban ecosystems. The ENA results demonstrate stronger ecological relationships compared to previous studies in this region [4], indicating intensifying interactions between different land use types. This suggests both challenges and opportunities for carbon metabolism management in rapidly urbanizing regions. By quantifying the carbon flows between different land use types, ENA provides a comprehensive framework for assessing the effectiveness of policy interventions and identifying areas for improvement. This methodological approach can be applied to other urban agglomerations to support the development of targeted carbon reduction strategies.

4.3. Policy Recommendations

Based on our findings, we propose several policy recommendations to enhance carbon metabolism and promote sustainable urban development in the BTHUA.

Firstly, there is a need for more stringent regulations of industrial and transportation land use to reduce carbon emissions, prioritizing compact urban development and promoting mixed-use zoning to reduce urban sprawl and its associated carbon footprint [64]. These could include the implementation of carbon pricing mechanisms and incentives for the adoption of low-carbon technologies [65].

Secondly, urban planning processes should prioritize the preservation and expansion of natural landscapes, such as forests and grassland, to enhance carbon sequestration.

This could be achieved through the establishment of green belts and the integration of green infrastructure into urban development projects [66,67]. At the same time, the government should implement stricter controls on urban expansion (e.g., the establishment of urban growth boundaries) while promoting compact city development to minimize carbon emissions from land use changes [68].

Thirdly, policymakers should consider the potential applicability of ENA in monitoring and evaluating the impacts of policy interventions on carbon metabolism. By providing a detailed understanding of carbon flows within urban ecosystems, ENA can support the development of more effective carbon reduction strategies and facilitate the alignment of local policies with national and international climate goals [69]. The government should enhance cooperation mechanisms between Beijing, Tianjin, and Hebei to achieve coordinated carbon reduction goals and prevent carbon leakage between jurisdictions. They can also incorporate carbon sequestration and emission targets into urban master plans and land use policies, ensuring that development decisions are aligned with climate change mitigation goals.

In general, this study highlights the critical role of policy implementation in shaping carbon metabolism in the BTHUA. By integrating ecological considerations into urban planning processes and leveraging advanced analytical tools like ENA, policymakers can develop targeted strategies to reduce carbon emissions and enhance carbon sequestration, contributing to the global fight against climate change. The alignment of our findings with national policies, particularly China's carbon neutrality goals, suggests that while progress has been made, more aggressive measures are needed to achieve substantial carbon reduction targets. Future policy frameworks should emphasize the integration of land use planning with carbon management strategies while considering the unique characteristics of different urban areas within the agglomeration.

5. Conclusions

This study constructed a network-based framework to assess the spatio-temporal dynamics of urban carbon metabolism associated with land use changes in the BTHUA, China. Our findings provide valuable insights into the dynamics of urban carbon metabolism and offer policy recommendations for sustainable urban development. The key findings are summarized below.

Industrial and transportation land had the highest carbon emission density, while forest land exhibited the highest carbon sequestration density. The negative net horizontal carbon flow indicated that land use changes exacerbated the disorder of carbon metabolism. The ecological relationships in the BTHUA were predominantly characterized by restriction and predation, with competition mainly present in the urban area. The increasing mutualism index (M) suggested a reduction in the negative impact of land use changes on carbon metabolism. The mutualism between positive carbon metabolism compartments, such as forest, grassland and water bodies, indicated that spatial planning played an essential role in transforming ecological relationships and enhancing carbon efficiency.

This study has certain limitations that should be acknowledged. For example, we did not explore the driving mechanisms of urban carbon metabolism and ecological relationship changes and lacked a quantitative analysis of the impacts of policies and management on the urban carbon metabolism. Despite these limitations, the findings underscore the complex ecological relationships within the BTHUA and highlight the necessity for strategic land use management to enhance carbon sequestration and mitigate the adverse effects of urban development on carbon metabolism. The methodology employed in this study can be applied to other urban agglomerations facing similar challenges.

Future research should focus on incorporating more detailed carbon flow data and considering the impact of technological innovation on carbon metabolism. Additionally, the development of more sophisticated monitoring systems and real-time carbon tracking mechanisms would enhance the effectiveness of carbon management strategies. Besides that, future research should focus on refining the methods for analyzing the interactions

between urban land use changes and carbon metabolism, particularly in the context of rapid urbanization and climate change mitigation strategies. In conclusion, while this study provides valuable insights into the carbon metabolism dynamics influenced by land use changes in the BTHUA, it also highlights the need for continued research and policy development to achieve a more sustainable and carbon-neutral urban future.

Author Contributions: Conceptualization, F.X.; methodology, F.X.; software, F.X. and X.G.; validation, F.X.; formal analysis, F.X.; investigation, F.X. and X.G.; resources, F.X.; data curation, F.X. and X.G.; writing, F.X. and X.G.; writing—review and editing, F.X.; visualization, F.X. and X.G.; supervision, F.X.; project administration, F.X.; funding acquisition, F.X. All authors have read and agreed to the published version of the manuscript.

Funding: This research was fully sponsored by the MOE (Ministry of Education in China) Project of Humanities and Social Sciences with grant number 23YJCZH252 and the Fundamental Research Funds for the Central Universities with grant number 2024SKQ08.

Data Availability Statement: The data presented in this study are available upon request from the corresponding author.

Conflicts of Interest: The authors declare no conflicts of interest.

References

1. Masson-Delmotte, V.; Zhai, P.; Pirani, A.; Connors, S.L.; Péan, C.; Chen, Y.; Goldfarb, L.; Gomis, M.I.; Matthews, J.B.R.; Berger, S.; et al. Climate change 2021: The physical science basis. *Contrib. Work. Group I Sixth Assess. Rep. Intergov. Panel Clim. Change* **2021**, *2*, 2391.
2. Piao, S.; Yue, C.; Ding, J.; Guo, Z. Perspectives on the role of terrestrial ecosystems in the 'carbon neutrality' strategy. *Sci. China Ser. D Earth Sci.* **2022**, *65*, 1178–1186. [CrossRef]
3. Wu, Y.; Shen, J.; Zhang, X.; Skitmore, M.; Lu, W. The impact of urbanization on carbon emissions in developing countries: A Chinese study based on the U-Kaya method. *J. Clean. Prod.* **2016**, *135*, 589–603. [CrossRef]
4. Zhou, L.; Zhou, C.; Che, L.; Wang, B. Spatio-temporal evolution and influencing factors of urban green development efficiency in China. *J. Geogr. Sci.* **2020**, *30*, 724–742. [CrossRef]
5. Wang, C.; Liu, H.; Zhang, M.; Wei, Z. The border effect on urban land expansion in China: The case of Beijing-Tianjin-Hebei region. *Land Use Policy* **2018**, *78*, 287–294. [CrossRef]
6. Xia, C.; Li, Y.; Ye, Y.; Shi, Z.; Liu, J.; Li, X. Analyzing urban carbon metabolism based on ecological network utility: A case study of Hangzhou City. *Acta Ecol. Sin.* **2018**, *38*, 73–85. (In Chinese)
7. Roadmap and Energy Development Prospect for Peaking Carbon Neutrality in Beijing-Tianjin-Hebei Region. Available online: https://ex.bjx.com.cn/html/20230105/42463.shtml (accessed on 5 June 2024).
8. The Beijing-Tianjin-Hebei Region and Its Surrounding Areas Have High Emission Intensity, Unreasonable Emission Structure and Distribution, and It Will Take a Long Time to Control Pollution. Available online: https://www.mee.gov.cn/ywgz/dqhjbh/dqhjzlgl/202003/t20200328_771502.shtml (accessed on 4 June 2024).
9. Du, J.; Fu, J.; Hao, M. Analyzing the carbon metabolism of "Production-Living-Ecological" space based on ecological network utility in Zhaotong. *J. Nat. Resour.* **2021**, *36*, 1208–1223. (In Chinese) [CrossRef]
10. De Carvalho, R.M.; Szlafsztein, C.F. Urban vegetation loss and ecosystem services: The influence on climate regulation and noise and air pollution. *Environ. Pollut.* **2019**, *245*, 844–852. [CrossRef] [PubMed]
11. Cui, X.; Li, S.; Gao, F. Examining spatial carbon metabolism: Features, future simulation, and land-based mitigation. *Ecol. Model.* **2020**, *438*, 109325. [CrossRef]
12. Houghton, R.A.; Hackler, J.L.; Lawrence, K.T. The US carbon budget: Contributions from land-use change. *Science* **1999**, *285*, 574–578. [CrossRef]
13. Sitch, S.; Smith, B.; Prentice, I.C.; Arneth, A.; Bondeau, A.; Cramer, W.; Kaplan, J.O.; Levis, S.; Lucht, W.; Sykes, M.T.; et al. Evaluation of ecosystem dynamics, plant geography and terrestrial carbon cycling in the LPJ dynamic global vegetation model. *Glob. Change Biol.* **2003**, *9*, 161–185. [CrossRef]
14. Hurtt, G.C.; Pacala, S.W.; Moorcroft, P.R.; Caspersen, J.; Shevliakova, E.; Houghton, R.A.; Moore Iii, B. Projecting the future of the US carbon sink. *Proc. Natl. Acad. Sci. USA* **2002**, *99*, 1389–1394. [CrossRef]
15. 2006 IPCC Guidelines for National Greenhouse Gas Inventories. Available online: https://www.ipcc-nggip.iges.or.jp/meeting/pdfiles/Washington_Report.pdf (accessed on 12 April 2024).
16. Page, J.; Kåresdotter, E.; Destouni, G.; Pan, H.; Kalantari, Z. A more complete accounting of greenhouse gas emissions and sequestration in urban landscapes. *Anthropocene* **2021**, *34*, 100296. [CrossRef]
17. Kennedy, C.; Steinberger, J.; Gasson, B.; Hansen, Y.; Hillman, T.; Havránek, M.; Pataki, D.; Phdungsilp, A.; Ramaswami, A.; Mendez, G.V. Methodology for inventorying greenhouse gas emissions from global cities. *Energy Policy* **2010**, *38*, 4828–4837. [CrossRef]

18. Cui, X.L.; Wei, X.Q.; Liu, W.; Zhang, F.; Li, Z.H. Spatial and temporal analysis of carbon sources and sinks through land use/cover changes in the Beijing-Tianjin-Hebei urban agglomeration region. *Phys. Chem. Earth* **2019**, *110*, 61–70. [CrossRef]
19. Chen, Q.; Su, M.; Meng, F.; Liu, Y.; Cai, Y.; Zhou, Y.; Yang, Z. Analysis of urban carbon metabolism characteristics based on provincial input-output tables. *J. Environ. Manag.* **2020**, *265*, 110561. [CrossRef]
20. Zhang, Y.; Wu, Q.; Fath, B.D. Review of spatial analysis of urban carbon metabolism. *Ecol. Model.* **2018**, *371*, 18–24. [CrossRef]
21. Zhang, Y.; Xia, L.; Xiang, W. Analyzing spatial patterns of urban carbon metabolism: A case study in Beijing, China. *Landsc. Urban Plan.* **2014**, *130*, 184–200. [CrossRef]
22. Borrett, S.R.; Scharler, U.M. Walk partitions of flow in Ecological Network Analysis: Review and synthesis of methods and indicators. *Ecol. Indic.* **2019**, *106*, 105451. [CrossRef]
23. Chen, B.; Chen, G. Urban energy consumption: Different insights from energy flow analysis, input–output analysis and ecological network analysis. *Appl. Energy* **2015**, *138*, 99–107. [CrossRef]
24. Burns, T.P.; Higashi, M.; Wainright, S.C.; Patten, B.C. Trophic unfolding of a continental shelf energy-flow network. *Ecol. Model.* **1991**, *55*, 1–26. [CrossRef]
25. Xia, L.; Fath, B.D.; Scharler, U.M.; Zhang, Y. Spatial variation in the ecological relationships among the components of Beijing's carbon metabolic system. *Sci. Total Environ.* **2016**, *544*, 103–113. [CrossRef]
26. Liu, G.; Casazza, M.; Hao, Y.; Zhang, Y.; Ulgiati, S. Emergy analysis of urban domestic water metabolism: A case study in Beijing (China). *J. Clean. Prod.* **2019**, *234*, 714–724. [CrossRef]
27. Han, H.; Guo, L.; Zhang, J.; Zhang, K.; Cui, N. Spatiotemporal analysis of the coordination of economic development, resource utilization, and environmental quality in the Beijing-Tianjin-Hebei urban agglomeration. *Ecol. Indic.* **2021**, *127*, 107724. [CrossRef]
28. Ren, X.; Xiong, R.; Ni, T. Spatial network characteristics of carbon balance in urban agglomerations–a case study in Beijing-Tianjin-Hebei city agglomeration. *Appl. Geogr.* **2024**, *169*, 103343. [CrossRef]
29. CNBS (China National Bureau of Statistics). *China Statistical Yearbook 2024*; China Statistics Press: Beijing, China, 2024.
30. Xu, X. *China's Multi-Period Land Use Land Cover Remote Sensing Monitoring DataSet (CNLUCC)*; Resource and Environment Data Science and Data Center, Chinese Academy of Sciences: Beijing, China, 2018.
31. Beijing Municipal Bureau of Statistics. *Beijing Statistical Yearbook 2001*; China Statistics Press (CSP) Publishing: Beijing, China, 2001.
32. Beijing Municipal Bureau of Statistics. *Beijing Statistical Yearbook 2011*; China Statistics Press (CSP) Publishing: Beijing, China, 2011.
33. Beijing Municipal Bureau of Statistics. *Beijing Statistical Yearbook 2021*; China Statistics Press (CSP) Publishing: Beijing, China, 2021.
34. Tianjin Municipal Bureau of Statistics. *Tianjin Statistical Yearbook 2001*; China Statistics Press (CSP) Publishing: Beijing, China, 2001.
35. Tianjin Municipal Bureau of Statistics. *Tianjin Statistical Yearbook 2011*; China Statistics Press (CSP) Publishing: Beijing, China, 2011.
36. Tianjin Municipal Bureau of Statistics. *Tianjin Statistical Yearbook 2021*; China Statistics Press (CSP) Publishing: Beijing, China, 2021.
37. Hebei Municipal Bureau of Statistics. *Hebei Statistical Yearbook 2001*; China Statistics Press (CSP) Publishing: Beijing, China, 2001.
38. Hebei Municipal Bureau of Statistics. *Hebei Statistical Yearbook 2011*; China Statistics Press (CSP) Publishing: Beijing, China, 2011.
39. Hebei Municipal Bureau of Statistics. *Hebei Statistical Yearbook 2021*; China Statistics Press (CSP) Publishing: Beijing, China, 2021.
40. Chen, P.; Wang, X.; Wang, L. *Carbon Budget and Its Sink Promotion of Terrestrial Ecosystem in China*; Science Press: Beijing, China, 2008. (In Chinese)
41. Fang, J.; Guo, Z.; Piao, S.; Chen, A. carbon sequestrations estimation of Chinese terrestrial vegetation from 1981 to 2000. *Sci. China (Ser. D Earth Sci.)* **2007**, *37*, 804–812.
42. Kong, D.; Zhang, H. Evaluation on the value of carbon sequestration function in the Heihe wetland national nature reserve in Zhangye. *Wetl. Sci.* **2014**, *12*, 29–34. (In Chinese)
43. Lai, L.; Huang, X.; Liu, W.; Zhao, D. Adjustment for regional ecological footprint based on input-output technique:A case study of Jiangsu Province in 2002. *Acta Ecol. Sin.* **2006**, *26*, 1285–1292. (In Chinese)
44. Piao, S.; Fang, J.; Zhou, L.; Zhu, B.; Tan, K.; Tao, S. Changes in vegetation net primary productivity from 1982 to 1999 in China. *Glob. Biogeochem. Cycles* **2005**, *19*. [CrossRef]
45. 2019 Refinement to the 2006 IPCCGuidelines for National Greenhouse Gas Inventories. Available online: https://www.ipcc.ch/report/2019-refinement-to-the-2006-ipcc-guidelines-for-national-greenhouse-gas-inventories/ (accessed on 15 April 2024).
46. She, W.; Huang, H.; Guan, C.; Chen, F.; Chen, G. The current carbon sequestration structure of China's staple crop production and its optimization approach. *Strateg. Study CAE* **2016**, *18*, 114–122. (In Chinese)
47. Zou, K.; Shu, Y.; Li, G.; Yan, Q.; Bo, Y.; Zhang, S.; Zhang, D. Urban Land-carbon Framework Construction Based on Ecological Network Analysis and Its Space-time Evolution Research. *J. Ecol. Rural. Environ.* **2022**, *38*, 972–982. (In Chinese)
48. Wei, J.; Xia, L.; Chen, L.; Zhang, Y.; Yang, Z. A network-based framework for characterizing urban carbon metabolism associated with land use changes: A case of Beijing city, China. *J. Clean. Prod.* **2022**, *371*, 133695. [CrossRef]
49. Zhang, Y.; Xia, L.; Fath, B.D.; Yang, Z.; Yin, X.; Su, M.; Liu, G.; Li, Y. Development of a spatially explicit network model of urban metabolism and analysis of the distribution of ecological relationships: Case study of Beijing, China. *J. Clean. Prod.* **2016**, *112*, 4304–4317. [CrossRef]
50. CNBS (China National Bureau of Statistics). *China Energy Statistical Yearbook 2020*; China Statistics Press: Beijing, China, 2020.
51. Finn, J.T. Flow analysis of models of the Hubbard Brook ecosystem. *Ecology* **1980**, *61*, 562–571. [CrossRef]
52. Fath, B.D. Network mutualism: Positive community-level relations in ecosystems. *Ecol. Model.* **2007**, *208*, 56–67. [CrossRef]
53. Liu, X.; Yu, L.; Si, Y.; Gong, P.; Wang, J. China's land cover and land use change from 1990 to 2010. *Sci. China Ser. D Earth Sci.* **2019**, *62*, 1418–1432.

54. Zhang, Y.; Zhang, J. Estimating the impacts of emissions trading scheme on low-carbon development. *J. Clean. Prod.* **2019**, *238*, 117913. [CrossRef]
55. Van der Heijden, J. Studying urban climate governance: Where to begin, what to look for, and how to make a meaningful contribution to scholarship and practice. *Earth Syst. Gov.* **2019**, *1*, 100005. [CrossRef]
56. Liu, Y.; Wang, Y. Integrating ecological and socioeconomic factors in land use planning: A comprehensive approach. *Environ. Sci. Policy* **2021**, *118*, 118–127.
57. Wang, J.; Chen, Y. The impact of ecological redline policy on land use and ecosystem services. *Land Use Policy* **2020**, *97*, 104780.
58. Chen, Y.; Zhang, S.; Yang, L.; Zhang, X.; Yu, K.; Li, J. Ecological footprint in Beijing-Tianjin-Hebei urban agglomeration: Evolution characteristics, driving mechanism, and compensation standard. *Environ. Impact Assess. Rev.* **2024**, *109*, 107649. [CrossRef]
59. Li, Y.; Shen, J.; Xia, C.; Xiang, M.; Cao, Y.; Yang, J. The impact of urban scale on carbon metabolism--a case study of Hangzhou, China. *J. Clean. Prod.* **2021**, *292*, 126055. [CrossRef]
60. Wang, H.; Zhang, X.; Zhang, X.; Liu, R.; Ning, X. Understanding coordinated development through spatial structure and network robustness: A case study of the Beijing-Tianjin-Hebei region. *J. Geogr. Sci.* **2024**, *34*, 1007–1036. [CrossRef]
61. Hu, T.; Li, X.; Gong, P.; Yu, W.; Huang, X. Evaluating the effect of plain afforestation project and future spatial suitability in Beijing. *Sci. China Ser. D Earth Sci.* **2020**, *63*, 1587–1598. [CrossRef]
62. Wang, K.; Ma, H. Does urban technological innovation and cooperation promote its green development? Evidence from cities in the Beijing-Tianjin-Hebei urban agglomeration, China. *J. Geogr. Sci.* **2024**, *34*, 1977–2002. [CrossRef]
63. Jamion, N.A.; Lee, K.E.; Mokhtar, M.; Goh, T.L.; Simon, N.; Goh, C.T.; Bhat, I.U.H. The integration of nature values and services in the nature-based solution assessment framework of constructed wetlands for carbon-water nexus in carbon sequestration and water security. *Environ. Geochem. Health* **2023**, *45*, 1201–1230. [CrossRef] [PubMed]
64. Liu, T.; Ji, Z.; Duan, Y.; Xu, Y. Spatial pattern evolution and carbon effect of production-living-ecological space in Zhangjiakou city under carbon peak and carbon neutrality goals. *Acta Sci. Nat. Univ. Pekin.* **2023**, *59*, 513–522. (In Chinese)
65. Zhang, Y.; Zhao, X.; Gong, J.; Luo, F.; Pan, Y. Effectiveness and driving mechanism of ecological restoration efforts in China from 2009 to 2019. *Sci. Total Environ.* **2024**, *910*, 168676. [CrossRef] [PubMed]
66. Liu, Z.; Deng, Z.; He, G.; Wang, H.; Zhang, X.; Lin, J.; Qi, Y.; Liang, X. Challenges and opportunities for carbon neutrality in China. *Nat. Rev. Earth Environ.* **2022**, *3*, 141–155. [CrossRef]
67. Wu, Y.; Wei, Y.; Liu, M.; García, I. Green infrastructure inequality in the context of COVID-19: Taking parks and trails as examples. *Urban For. Urban Green.* **2023**, *86*, 128027. [CrossRef]
68. Pan, X.; Liu, Z.; He, C.; Huang, Q. Modeling urban expansion by integrating a convolutional neural network and a recurrent neural network. *Int. J. Appl. Earth Obs. Geoinf.* **2022**, *112*, 102977. [CrossRef]
69. Wang, N.; Chen, X.; Zhang, Y.; Pang, J.; Long, Z.; Chen, Y.; Zhang, Z. Integrated effects of land use and land cover change on carbon metabolism: Based on ecological network analysis. *Environ. Impact Assess. Rev.* **2024**, *104*, 107320. [CrossRef]

Disclaimer/Publisher's Note: The statements, opinions and data contained in all publications are solely those of the individual author(s) and contributor(s) and not of MDPI and/or the editor(s). MDPI and/or the editor(s) disclaim responsibility for any injury to people or property resulting from any ideas, methods, instructions or products referred to in the content.